# Chapter 3
# Characterization of Bacterial Adhesion and Biofilm Formation

**Nil Tandogan, Pegah N. Abadian, Bowen Huo, and Edgar D. Goluch**

## 3.1 Introduction

For well over 100 years, researchers have been growing bacteria in test tubes as liquid cultures and on petri dishes as colonies. These two approaches have provided us with a wealth of information; however, they are of limited value for studying bacterial adhesion and biofilm formation. We are now aware of the significant cellular and molecular-level differences between planktonic and adherent cells that necessitate new strategies for generating and characterizing biofilms [1]. Biofilms are a crucial survival mechanism for bacteria. As it is now well known, bacterial cells become more virulent and more resistant to antibiotics when they are inside of a biofilm. Hence, patients with chronic infections are often suspected of having a biofilm that prolongs their recovery.

Further complicating the situation is the fact that the properties of biofilms and the cells inside of them change with time and environmental conditions. For example, cells exposed to certain flow geometries will generate biofilms, known as streamers that extend far away from the attachment point and cause severe problems in pipelines [2, 3]. In other flow profiles, such as ship exteriors, the same species of bacteria can form biofilms that are extremely adherent, increasing the drag force and corroding the surface. Biofilms are not always virulent and destructive. Some bacteria involved in nutrient cycling and biodegradation form biofilms at the air/water interface [4–7]. As you can imagine, many different techniques are required to study all of the various types of biofilms.

We will first discuss each stage of biofilm formation in some detail, and then we will focus on characterization methods and how they are used to analyze various stages of the biofilm life cycle.

N. Tandogan • P.N. Abadian • B. Huo • E.D. Goluch (✉)
Department of Chemical Engineering, Northeastern University, Boston, MA 02115, USA
e-mail: E.Goluch@northeastern.edu



Z. Zhang, V.E. Wagner (eds.), *Antimicrobial Coatings and Modifications on Medical Devices*, DOI 10.1007/978-3-319-57494-3_3

## 3.2 Biofilm Life Cycle

Biofilms were first analyzed in the 1930s. One of the first biofilm studies was reported by Henrici et al. who described the process of biofilm formation as "The deposit of bacteria becomes apparent in a few days and increases progressively, eventually becoming so thick that individual cells may be distinguished with difficulty. That the cells are actually growing upon the glass is indicated by their occurrence in microcolonies of steadily increasing size. They are fairly firmly adherent to the glass, not removed by washing under a tap." This description highlights the three main components required to identify a biofilm: bacterial cells, an extracellular matrix, and a surface or interface [8]. Other factors, such as environmental conditions and cell-to-cell signaling, affect the properties of the biofilm.

Biofilm formation begins with initial weak interactions between individual bacterial cells and the surface, followed by a strong adhesion step. The cells then begin to excrete various biomolecules, which are collectively referred to as extracellular polymeric substance (EPS), as they grow and divide. The EPS matrix significantly increases the robustness of the biofilm. The biofilm reaches a maximum size and enters a stasis stage during which it is referred to as "mature." In the final stage, cells detach from the biofilm and move to new locations [9, 10]. A schematic of the process is shown in Fig. 3.1.

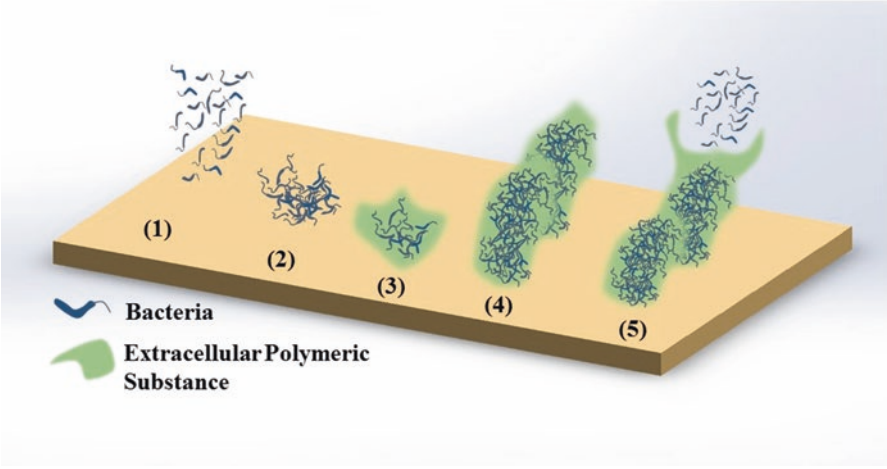


**Fig. 3.1** The stages of a biofilm: (*1*) reversible attachment of bacterial cells, (*2*) irreversible attachment of the cells, (*3*) production of extracellular polymeric substance, (*4*) maturation of the biofilm, and (*5*) dispersal of bacterial cells from the biofilm

### *3.2.1 Adhesion*

Biofilm formation starts with the adhesion of cells to a surface. As bacterial cells swim, or move in their environment by Brownian motion, they continuously sense and assess chemical cues through receptors embedded in their membranes. Adhesion to surfaces is advantageous for bacteria, as it provides access to nutrients precipitated on surfaces and protection from predators and environmental hazards [11, 12]. Since they have such a significant impact on survival, the mechanisms bacteria use to initiate adhesion to surfaces have been an important subject of many studies.

Bacterial adhesion to surfaces starts with initial weak attractions, which are reversible and can be broken fairly easily, using, for example, an increase in fluid shear. There are three theories that incorporate chemical interactions and thermodynamic principles to predict the possibility of reversible adhesion to surfaces. Once the weak adhesion is achieved, stronger chemical bonds form and bacteria secrete polymeric substances to strengthen the adhesion. We will now cover the steps in detail.

#### 3.2.1.1 Reversible, Weak Adhesion

The theories that explain the reversible bonding mechanism, which initiates the adhesion process, are the DLVO (Derjaguin, Landau, Verwey, Overbeek) theory of colloid stability, the thermodynamic approach, and the extended DLVO [13]. In this section, we provide an introduction to each of the theories, which are frequently used for analyzing cell adhesion and biofilm formation. More in-depth explanations are provided in the referenced papers [13–16].

#### 3.2.1.2 DLVO Theory

The DLVO theory of colloid stability employs the change in Gibbs free energy between colloid particles and surfaces as a function of distance and has been used to explain the reversible interactions between bacterial cells and surfaces, as bacteria can be approximated as large colloidal particles. The theory quantitatively describes the initial reversible interactions between bacteria and surfaces by summing the attractive hydrophobic Van der Waals bonds and repellent Coulomb double layer interactions, which occur due to charges on bacterial membrane and the surface [17]. DLVO does not take into account steric hindrance or hydrogen bond formation; however, these phenomena occur when the separation distance is less than 1 nm [18]. Adhesive forces between bacteria and surfaces have been measured when the two are as far as 20 nm apart, demonstrating the value of DLVO theory [19]. When the separation distance between bacteria and surface becomes less than 1 nm, steric hindrance and hydrogen bonds start to form, and DLVO theory is no longer applicable [20].

As planktonic bacterial cells swim or randomly move around via Brownian motion, they sense and approach within a few nanometers of the surface. Depending on their distance from the surface, their interaction with it varies. Van der Waals bonds are very weak hydrophobic interactions formed between the cell and the surface. The weakness of the bonds gives flexibility to bacterial cells as they can still exhibit Brownian motion and be detached from the surface when exposed to mild shear stress [18]. Coulomb interactions depend on the amount of charge on the bacterial cell membrane and the surface. Both Gram-positive and Gram-negative bacteria carry negative charges on their membrane [21, 22]. Teichoic acids embedded on the peptidoglycan wall of Gram-positive bacteria give the cells a net negative charge; while the lipopolysaccharides (LPS) on the outer membrane of Gram-negative bacteria are responsible for their net negative surface charge. In nature, surfaces also have negative charges. Hence, the Coulomb interactions are repellent, but the intensity varies with the ionic strength of the electrolyte solution. As a cell approaches a charged surface, an electrical double layer forms between the cell and the surface, which consists of two parallel layers. The counter ions in the aqueous solution are attracted to the charges on the surface, creating the first layer. The second layer is comprised of the free ions in the solution that are attracted to the bacterial membrane. Repulsion occurs when the electrical double layers overlap [23]. As the concentration of counter ions increases and interacts with the negatively charged surface, the electrostatic double layer thickness (the inverse Debye length) on the surface decreases, changing the net attraction to positive and thus promotes bacterial adhesion [20].

Beyond this ionic energy barrier, there is a second energy minimum, and its distance from the surface varies with the ionic strength of the sample solution, as shown in Fig. 3.2 [24]. Bacteria can reach this second energy minimum by using their appendages or by secreting extracellular polymeric substance (EPS) to adhere to the surface reversibly. As the contact radius decreases, the secondary energy minimum is lowered and adhesion can be induced [23]. At low ionic strength, however, the thickness of the electrical double layer increases; thus bacterial EPS or appendages cannot pass through the secondary energy minimum and reach the sur-

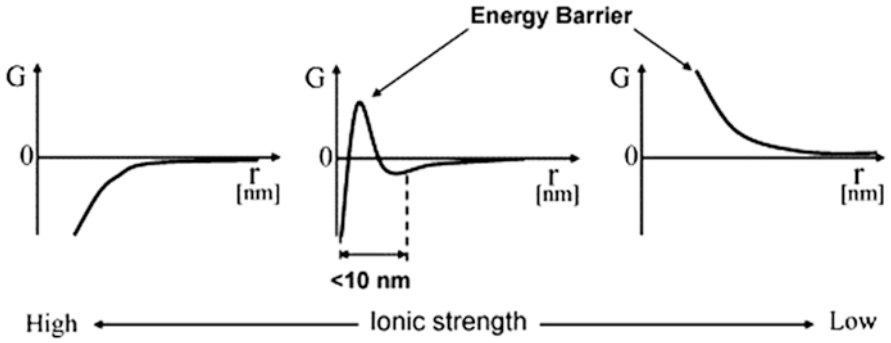


**Fig. 3.2** Effect of ionic strength on total interaction energy between a bacterial cell and a surface (Adapted with permission from Ref. [24])

face. The secondary energy minimum is therefore an important part of the early reversible interactions exhibited by bacteria. Redman et al. experimentally demonstrated this phenomenon by flowing *E. coli* through a packed bed column with quartz grains as porous media [25].

Concerning the properties of bacterial cell membranes, DLVO theory does not account for several factors that play a role in the adhesion process. Hydrophobicity is one such factor. Rijnaarts et al. demonstrated that bacteria adhered more to hydrophobic Teflon surfaces than to glass [26]. This parameter is particularly important in wastewater treatment plants. Zita et al. showed that surface hydrophobicity promotes adhesion to sludge flocs in wastewater treatment processes [27]. In another work, the authors used fluorescent microspheres that could attach to the membrane surface of bacteria to measure the hydrophobicity of the bacterial cell surface, and their results indicated that the majority of bacteria showed hydrophilic membrane surface properties [28]. Van Loosdrecht et al. employed a more common approach, contact angle measurement, which we will discuss later in this chapter, to determine cell surface hydrophobicity and reported that the cellular growth phase affects the hydrophobicity of bacterial cells and biofilms [29]. It is important to note that depending on the species, bacterial cells can vary significantly between being hydrophobic or hydrophilic. DLVO theory also does not consider steric interactions between bacterial cells and the surface.

#### 3.2.1.3 Thermodynamic Theory

Thermodynamic theory is another approach to explain the possibility of reversible interactions between bacteria and surfaces. This theory assumes that the interactions are always reversible, so it cannot be used to explain irreversible interactions [24]. The theory uses the Dupré equation, which evaluates the changes in free energy of adhesion using the interfacial free energy in the substrate microorganisms, aqueous phase microorganism, and substrate aqueous phases [23]. The basic thermodynamic principle utilized is that the system will always favor the minimum free energy conditions. This is also the case when determining the initial adhesion behavior of bacteria. The theory employs a very simple premise: bacterial adhesion should only be observed when the change in free energy is negative [13, 30].

Experimentally, surface energy or surface tension can be estimated via contact angle measurement, which is a common technique to predict the wettability of a surface. In one such example, Qu et al. analyzed the adhesion of bacterial species *Pseudomonas aeruginosa* (*P. aeruginosa*), *Staphylococci*, and *Serratia* to different contact lenses using thermodynamic approach. They calculated interfacial free energies from the contact angles [31]. As thermodynamically expected, they noted that bacterial adhesion is greater as the change in interfacial free energies is more negative. However, there are several studies where the thermodynamic approach led to contradictory results, when compared to the experimental results [23, 32]. One limitation of the theory is that bacterial cells may contact the surface only through surface appendages with a very small contact region, which are not accounted for in thermodynamic theory.

#### 3.2.1.4 Extended DLVO

Both classic DLVO theory and the thermodynamic approach fail to explain interactions that could play a bigger role in bacterial adhesion, thus potentially resulting in misleading estimations of bacterial adhesion [33]. The classic DLVO theory only considers Van der Waals and electrostatic forces, and the thermodynamic approach only takes into account electrostatic interactions and interfacial free energies. Interactions, including Lewis acid-base, electron accepting/donating, and osmotic interactions, in some cases, can be the most important factors for determining bacterial adhesion characteristics [25, 34, 35]. Though these interactions require closer proximity to the surface than Van der Waals bonds or electrostatic interactions, they are stronger. For instance, Lewis acid-base interactions are one to two orders of magnitude stronger than electrostatic forces [36]. Van Oss proposed an extended version of DLVO, which estimates the changes in Gibbs energy of adhesion by including these interactions [36].

Sharma et al. evaluated all three approaches and compared them by experimentally testing the adhesion of *Paenibacillus polymyxa* bacteria onto minerals [33]. The results of this study revealed that the adhesion was governed primarily by Lewis acid-base interactions, which are accounted for in extended DLVO theory. Classic DLVO theory partially explained the observed behavior. The thermodynamic approach, however, predicted that no bacterial adhesion would occur.

Although extended DLVO approximations are relatively accurate, each case should be evaluated carefully, as there are cases, such as complex nanoscale structures on bacterial cell surfaces, that can make it difficult to explain the results even with extended DLVO [14]. Ong et al. illustrated the difficulties associated with modeling the bacterial adhesion process using extended DLVO theory when the cell surface contains complex structures [37]. A theory that takes into account all of the variables involved in bacteria adhesion would be quite complicated to derive and use, particularly as many of the factors are difficult to measure, but such a comprehensive theory would be incredibly beneficial to researchers working with bacteria in nearly every basic and applied field.

### *3.2.2 Surface Characteristics Affect Bacterial Adhesion*

Surface characteristics such as roughness, free energy, and hydrophobicity manipulate bacterial adhesion on surfaces. This has led many researchers to focus on altering the surface chemistry of substrates to deter bacterial attachment [38]. The addition of nanoparticles to surfaces and changes in the surface chemistry have been shown to deter bacterial attachment to surfaces [39–41]. Self-assembled monolayers (SAMs) also effectively alter bacterial adhesion properties, either enhancing or preventing them as needed. Liu et al. examined the interaction of *Staphylococcus epidermidis* (*S. epidermidis*) with different surface protein layers: fibronectin and fetal bovine serum (FBS) [15]. Calculation of Gibbs free energy values revealed that while the thermodynamic approach estimated bacterial adhesion to surfaces with

non-protein layers and FBS layers well, its estimation of adhesion strength of bacteria to fibronectin-covered surfaces was not as accurate, which could be due to strong interaction between *S. epidermidis* and fibronectin. Ista et al. tried SAMs terminated with different chemical groups, including hexa(ethylene glycol), methyl, carboxylic acid, and fluorocarbon on solid substrates and tested the attachment behavior of *S. epidermidis* and a marine species *Deleya marina*. While the two species showed different preferences for the hydrophilicity of the surface, the SAM with oligo(ethylene glycol) end group on the surface significantly prevented the attachment of both species [42]. In addition to ethylene glycol functional groups, Ostuni et al. focused on determining different SAMs that hinder the attachment of proteins, bacterial cells, and mammalian cells [43]. Among the SAMs they tested, they concluded that SAMs terminating with –tri(sarcosine), N-acetylpiperazine, and an intramolecular zwitterion prevented the adhesion of *S. aureus* and *S. epidermidis* as comparable as to SAMs ending with ethylene glycol.

### *3.2.3 Irreversible Adhesion and EPS Production*

Once bacterial cells have their initial contact with the surface, they continue to strengthen their attachment with irreversible bonds. In order to do so, they create a matrix of extracellular polymeric substances (EPS), which contains several complex polysaccharides, proteins, nucleic acids, and phospholipids [10]. EPS is the major component of a biofilm and provides numerous advantageous to cells. The structure immobilizes cells onto the surface, provides a robust shield against antibacterial agents, and creates a close network between the cells so that the cells can communicate with each other and exchange nutrients and other important molecules [44]. The structure of the matrix is very dynamic and complex, and its composition and morphology varies significantly between species. The structure can range from flat and smooth to rough and filamentous. Among the most common biofilm shapes are the mushroom-like structure of *P. aeruginosa* and the fruiting shape of *Myxococcus xanthus* [45].

In order to initiate the synthesis of numerous polymer blocks, significant modifications in gene expression occur. Several genes are turned on once the bacterial cells achieve their initial contact with the surface. The density of cells near the surface also affects gene regulation. As we mentioned earlier, bacterial cells continuously communicate with their environment and neighboring cells through self-signaling molecules. When the self-signaling molecules reach a certain threshold concentration, they activate genes that will express quorum sensing molecules (QSMs). QSMs regulate genetic expressions, modulate the synthesis of the EPS matrix, or induce virulence. The mechanism of quorum sensing has been widely studied. It was initially believed that quorum sensing starts only when a critical number of cells are present. However, advances in technology provided the opportunity to examine this phenomenon more closely at the single cell level [46]. Connell et al. created picoliter-sized microcavities and observed the quorum sensing behavior starting from a single cell [47]. Their results suggested that bacterial cells could

start processes for developing antibiotic resistance, which are also a quorum sensing response, with only 150 cells. Cell density therefore becomes the critical factor when the cell number is low.

QSMs are believed to begin playing a role in the regulation of cell function only after cell adhesion takes place [48], thus marking a distinct stage in the biofilm life cycle. To test this theory, wild-type *P. aeruginosa* cells were compared to the ones that had a mutation in a gene that controls cell-to-cell signaling. The results showed that while both cell types attached to the surface, the wild-type cells formed thick biofilms, whereas the mutated ones formed only a thin sheet of growth. Davies et al. investigated changes in the genetic regulation of alginate biosynthesis pathway between planktonic and biofilm *P. aeruginosa* cells. Alginate is one of the well-studied constituents of the EPS matrix, and their results indicated that the genes associated with alginate synthesis were upregulated after planktonic cells attached to a surface [49, 50]. Hence, there is a distinction between cell adhesion and EPS production.

Other factors, including the adhesive appendages of bacterial species and gene expression, also contribute to the adhesion process [51]. The appendages, fimbriae, found in many species in *Enterobacteriaceae* family are specific to mannose groups which are present on human epithelial cells [52]. One example is that *E. coli* has pili with FimH adhesin at the tips that adheres to the mannose groups of oligosaccharides located on the surface of epithelial cells [53–55].

### *3.2.4 Biofilm Maturation, Disassembly, and Dispersal*

Bacterial cells producing EPS eventually create a biofilm that has a set size and shape for a given set of environmental conditions. A biofilm at this stage is referred to as being "mature." A mature biofilm is thought to be at steady state, where a balance is achieved between nutrient transport and cellular activity in the biofilm. The amount of time needed for a mature biofilm to form ranges from several hours to several weeks. Bacterial cells in a biofilm are known to differentiate their functions, with a fraction going dormant [56, 57]. The regulatory mechanism involved in the process of differentiation is not yet well understood, neither are the mechanisms by which the dormant cells are reactivated. When the protein expression of planktonic *P. aeruginosa* cells and the ones at the maturation stage in a biofilm was compared, expression of 50% of the entire proteome was increased sixfold, highlighting the complexity of cell activity at this stage and the potential for heterogeneity in cellular function [58].

The final stage of the biofilm life cycle is called disassembly or dispersal. In this stage, cells in the biofilm produce enzymes that dissolve the EPS, releasing them from the biofilm. Relatively little is known about the mechanisms that regulate biofilm disassembly and dispersal [59]. This knowledge gap for the final two stages of the biofilm life cycle is the result of two limitations. First, the experimental setup for growing large quantities of biofilms that have the reproducible physical and chemical properties is complicated relative to liquid and plate cultures. Second, it

is challenging to analyze what is happening to the biofilms and the cells inside of them as the processes of interest are dynamic, varying in both time and location within the biofilm. The new techniques that are being developed to address these analytical challenges are described in the next section of this chapter.

## 3.3 Techniques for Making Biofilms

Before we can analyze a biofilm, we must first create it. The specialized techniques, which are required for creating biofilms, are described in the following sub-sections.

### *3.3.1 Biofilm Reactors*

While biofilms grow in a variety of environmental conditions, one technique has become the standard for creating biofilms. The general approach is to seed bacteria on the surface of interest and then flow fluid past it. The cells grow on the surface and form a biofilm. Alternatively, the fluid can contain bacteria and the bacterial attachment and subsequent biofilm formation occur simultaneously while the fluid is flowing.

The Center for Biofilm Engineering (CBE) at Montana State University has created many of the instruments and protocols associated with bulk biofilm production and analysis during the last 25 years. One of the most used instruments is the CDC Biofilm Reactor, which allows various species of biofilms to grow on sample surfaces [60, 61]. The reactor is a vessel with rods that hold the biofilms extended outward into the fluid in the container (Fig. 3.3). The fluid is rotated, resulting in the application of shear to the biofilm, using a stir bar. The reactor is able to grow multiple biofilm samples under high shear stress simultaneously, and the biofilms can be harvested individually for testing. The CDC Biofilm Reactor is most frequently used to analyze biofilm removal. The biofilm is grown on a surface of interest. Then, the surface coated with biofilm is removed from the reactor and exposed to a cleaning solution. The biofilm is then removed from the surface using sonication and the eluent is tested for microbial growth using culture plates. The American Society for Testing and Materials has approved protocol E2562, which is a method for the quantification of *P. aeruginosa* biofilm growth using the CDC Biofilm Reactor [62]. The reactor has also been used to grow biofilms for in vivo implantation in animal studies [63]. The limitation of the reactor design is that it does not allow for in-line analysis of the biofilm.

Like the CDC Biofilm Reactor, the Drip Flow Reactor (DFR) was also developed by the CBE. The DFR grows biofilms under low shear stress conditions by dripping bacteria onto a slide, while the device is held at an angle to cause gravimetric flow [64]. The methods used for the DFR were accepted by the ATSM with the designation E2647. A schematic of the DFR is shown in Fig. 3.4. The DFR can be combined

**Fig. 3.3** Photograph of a 1 liter glass CDC Biofilm Reactor (Adapted with permission from Ref. [63])

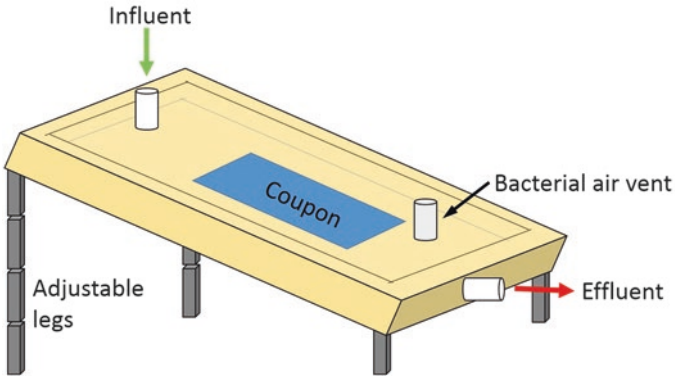


**Fig. 3.4** Schematic of a Drip Flow Reactor. The coupon is the material of interest on which the biofilm forms

with some microscopy setups to perform in-line analysis if the surface material (coupon) is transparent.

Liu et al. (2001) used their own annular reactor made of PVC to grow biofilms and observed that the biofilms were able to respond metabolically and physically change under shear stress [65]. In the reactor, the changes in shear stress affected the anabolism and catabolism rate as well as the density and size of the biofilm. However, this setup only showed a macroscopic effect on biofilms because the reactor volume was 4 L, which was much larger than the scale of bacteria. They were able to show that biofilm characteristics changed depending on the shear stress applied. As shear stress increased, the biofilms became smoother and denser [65]. The denser biofilm correlates to the finding of the DFR biofilm reactor, where biofilms grown under

lower shear stress were less tolerant to treatment methods [64]. These results highlight how shear stress not only affects the rate of formation but also the properties of the formed biofilm.

### 3.3.2 *Modified Microwell Plates*

Microwell, or microtiter, plates are a staple of microbiology research. Microwell plates allow from 6 to 1536 experiments to be performed simultaneously. One of the main benefits of using microwell plates for biofilm experiments is that the plates allow for in situ sample analysis. Foncesa et al. used a microwell plate assay to evaluate biofilm adhesion during antibiotic treatment [66]. Orbital shaking applied a shear force to create dynamic conditions for the assessment of biofilm adhesion. Their experiments began with planktonic bacteria and observed the adhesion and formation of the biofilm. They showed that under dynamic conditions, the antibiotic was more effective at preventing biofilm formation. This study successfully demonstrated that the combination of shear stress and a chemical treatment affected biofilm formation more than each one does individually.

The Calgary Biofilm Device (CBD), shown in Fig. 3.5, is the most important advancement to microwell plates that has been made for biofilm analysis. This device grows biofilms in a 96-well plate format, which can then be tested using standardized molecular and quantitative analysis techniques. The CBD has been used to demonstrate the differences between the removal of bacteria in biofilms and

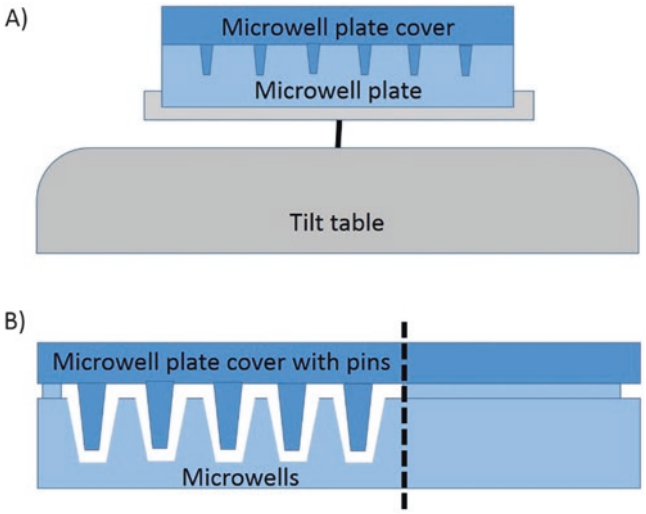


**Fig. 3.5** (**a**) A tilt table that creates shear during biofilm formation by rotating the microwell plate, which causes the fluid inside each microwell to move. (**b**) Cutaway view of a Calgary Biofilm Device (CBD) showing the pins sitting inside of the wells of the microwell plate

planktonic bacteria. Ceri et al. (1999) used the Calgary Biofilm Device (CBD) to test the susceptibility of biofilms to antibiotics [67]. They observed that antibiotic concentrations necessary to remove biofilms were 100 to 1000 times higher than concentrations to remove their planktonic counterparts. The CBD can further be combined with a phenotypic microarray to assess metabolic activity through the use of a dye [68]. However, the CBD only grows biofilms in a monolayer and cannot evaluate biofilms grown in multiple layers. Furthermore, the CBD does not combine chemical treatment with application of a shear.

Annular reactors are another method of evaluating biofilm removal, which can be monitored by using laser-based focused beam reflectance measurements. Choi et al. (2003) attempted to establish which detachment process dominates the removal of a biofilm subjected to fluid flow [69]. The use of annular reactors successfully determined that most of the biofilm removal due to shear stress was done through erosion, which is the transfer of small particles from the biofilm into the bulk fluid [69]. This result indicates that at steady state, gradual removal of the biofilm should be expected. While the annular reactors evaluated biofilm removal under shear stress, they were not used to evaluate the efficacy of chemical treatment.

The biofilms grown with both CBDs and DRF devices have been used to evaluate biofilm removal [62, 64]. Once the biofilms were grown in both devices, the sample surfaces were removed from the device and tested. The biofilms that were formed under higher shear stress were more resilient to treatment methods [64]. These results support the work done by Liu et al. (2001), where biofilms formed under higher shear stress were denser than biofilms formed under low shear stress [65]. The studies conducted by Ceri et al. and Choi et al. addressed chemical treatment and shear stress, respectively. By first growing a biofilm and then testing the properties of the biofilm, they ensured that they were testing the biofilm and not planktonic bacteria.

## 3.4 Techniques for Analyzing Adhesion and Biofilm Properties

We will now describe the techniques used for studying cell adhesion and biofilms. We group them unofficially into two categories: traditional and emerging. Traditional techniques primarily analyze the bulk properties of biofilms and assess the effectiveness of chemicals to kill cells in biofilms. These techniques generally focus on biofilms found in the outdoor environment and industrial settings. As the medical community became aware of biofilms and their role in human disease, a need has emerged for high-throughput analysis and techniques that measure the mechanisms involved in the biofilm life cycle. New high-tech approaches, such as microfluidics, label-free, and real-time sensors, are required to meet these requirements. Methods for high-throughput and mechanistic analysis are still primarily in the development stages and have not yet been adopted by industry or regulatory agencies, hence the “emerging” nomenclature.

### 3.4.1 Contact Angle Measurements

One of the first and simplest techniques for evaluating biofilm and surface properties is contact angle measurement. The contact angle is the angle between liquid-vapor and liquid-solid interfaces of the liquid-solid-vapor system, which can then be inserted into Young's equation to thermodynamically determine interfacial energies [70]. The wettability of the surface reveals information about its hydrophobicity [71]. Contact angles are measured by placing a drop of water on the surface of interest, which can be either the surface on which the bacterial cells will attach or on top of the biofilm after it has formed on the surface. The angle that the drop makes with the surface on the inside of the drop is measured optically as shown in Fig. 3.6. The angles above 90° indicate a non-wetting or a hydrophobic surface, whereas angles below 90° show wetting or hydrophilic surfaces [72]. In one such example, Wang et al. evaluated the hydrophobicity of *P. aeruginosa* PAO1, *Pseudomonas putida*, and *E. coli* by measuring the contact angles of DI water, ethylene glycol, and methylene iodide on bacterial lawn with a Rame-Hart Goniometer, and results elucidated that PAO1 is more hydrophobic than the other two strains [14]. It is worth noting that there are concerns over the accuracy of contact angle measurements for bacterial hydrophobicity, due to the experimental challenges, including the dehydration of the bacterial lawn and the number of bacterial layers needed for the measurements [73].

Two types of contact angles can be measured: static contact angle and dynamic contact angle. Static contact angle is the angle obtained when the liquid droplet is still on the surface, and the boundary of liquid–solid–vapor phases is stagnant, whereas the dynamic contact angle is measured when the three-phase boundary is changing. This could be either due to the change in volume of the droplet or the tilting of the liquid droplet. As a result of this change, the formed contact angles are called the receding and the advancing angles, and the contact angle lies between these two angles.

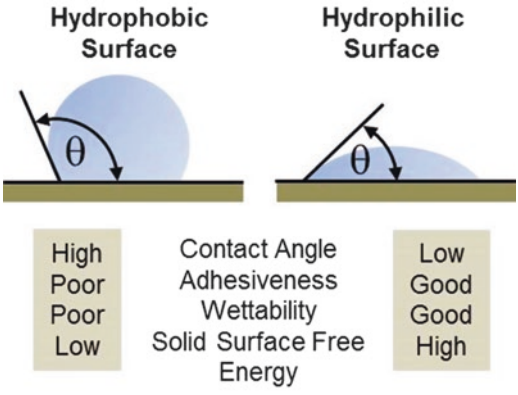


**Fig. 3.6** Contact angle measurements provide information about the hydrophobicity of clean surfaces and biofilms

### 3.4.2 Microscopy Techniques

Different microscopy techniques have been implemented to visualize and detect biofilms and bacterial cells. Selection of the right microscopy technique varies with the experimental setting and the level of information needed from the sample, since each technique provides different details depending on the magnification and resolution limitations of the microscopes. The following sections highlight the most widely applied microscopy techniques on biofilm studies.

### 3.4.3 Confocal Scanning Laser Microscopy (CLSM)

Several studies incorporate confocal scanning laser microscopy (CLSM) to visualize biofilms and to understand more about the EPS structure as it offers high-resolution images by optically sectioning the specimen into planes and scanning one plane at a time with laser illumination [74]. The specimen can be imaged without chemical fixation or dehydration, which makes this technique stand out from other methods with more destructive sample preparation steps. The sections are combined to construct a 3D model to obtain additional information from the sample, which is not possible with conventional fluorescence microscopy [75]. An example of a biofilm formed inside of a microfluidic channel that is imaged with CLSM is shown in Fig. 3.7.

Several groups have used confocal microscopy to construct three-dimensional images of a biofilm [76, 77]. Using CLSM, Lawrence et al. identified and compared the bacterial and EPS regions of biofilms among different species [78]. The biofilms they measured were hydrated and cells only account for 2–23% of the biofilm volume.

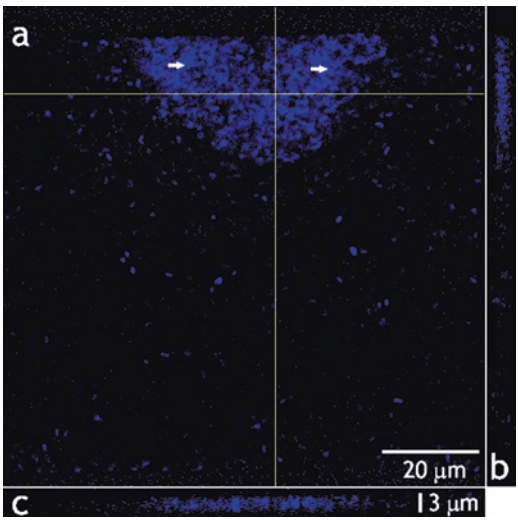


**Fig. 3.7** Confocal images of a biofilm inside of a microfluidic channel: (**a**) 3D projection, (**b**) yz cross section and (**c**) xy cross section. The cross sections were taken at the respective *yellow lines*. The *white arrows* indicate areas where bacterial cells are on top of each other

Caldwell et al. pioneered the use of CLSM for imaging bacterial cells and biofilms in the 1990s [79, 80]. The use of CLSM was followed by several other researchers, including Wood et al. illustrating of the structure of intact biofilm from human dental plaque [81], Kim et al. studying the effectiveness of antimicrobials on biofilm [82], and many more [83, 84]. One of the drawbacks of this technique, however, is the ability to damage cells with the high intensity of the laser beam. The complexity and cost of confocal systems have also limited their use thus far.

### *3.4.4 Molecular Methods*

There are numerous molecular techniques that can be coupled with microscopy to learn about how individual cells function in biofilms. Commonly used techniques include gene chips, fluorescent tagging, and fusion proteins. We will not go into the details of these techniques here, as they are applicable to all cellular analysis and generally do not require modification for bacterial research.

### *3.4.5 Atomic Force Microscopy (AFM)*

AFM is a scanning probe technique that provides information about the surface properties of a sample, including topography, roughness, and height at sub-nanometer scale resolution. For bacterial cells and biofilms, it is a great method for determining membrane structure, stiffness, adhesion characteristics, and even observing cellular growth and division in 3D (Fig. 3.8) [85–88]. A major advantage of AFM is that it requires minimal sample preparation such as no chemical treatments to fix or dehydrate cells as it runs at atmospheric conditions. Thus it elucidates a more realistic profile regarding biofilms and allows real-time imaging of live cells at very high resolution. Nevertheless, it is often necessary to use linkers such

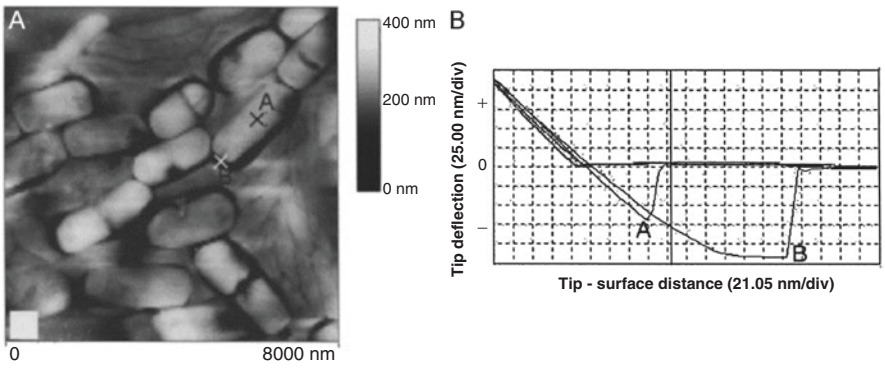


**Fig. 3.8** (**a**) AFM image of a developing biofilm of sulfate-reducing bacteria, (**b**) force–distance curves at locations *A* and *B* (Adapted from Ref. [86])

as poly L-lysine to immobilize cells, particularly the motile cells, to surfaces, or porous membranes to trap cells. Information is gathered by detecting the oscillations of a cantilever as the surface topography changes. On the tip of a cantilever, there is a sharp probe and as it scans the surface of a sample, the forces between the probe and the sample lead to oscillations on the cantilever. These oscillations are measured with photodiodes by detecting the movement of a laser beam that is reflected off of the cantilever [89].

Information about the sample can be collected using different AFM modes: contact mode and tapping mode. Contact mode is the most extensively used mode to analyze bacterial cells and biofilms. As the name implies, the probe contacts the specimen while it scans the surface. The interaction between the specimen and the probe, however, causes drag forces, which can alter or damage the specimen [90]. Tapping mode is an alternative mode that scans the surface by briefly contacting the specimen at a very high frequency. The brief contact avoids the drag forces between the probe and the specimen and minimizes damage to the sample [87].

One example application of AFM is a series of studies of composite materials used in dental procedures to investigate their interaction with bacteria [91–94]. The effect of surface roughness on the adhesion of *Streptococci* onto dental composite resins was investigated in a study by changing the roughness of the composite resins [95]. Not only is the roughness of the surface determined using AFM, but the strength of the adhesion of bacterial cells onto the surface can also be measuring with AFM. Analysis of the adhesion forces showed that the roughness of the surface increases the adhesion, and the adhesion forces vary with bacterial species.

Another study focused on the adhesion of *P. aeruginosa* on fungi *Candida albicans* (*C. albicans*) [96]. Authors analyzed the surface thermodynamics, tested surface interactions with AFM, and concluded that the mannoprotein layer expressed on *C. albicans* allows initial acid–base and Van der Waals interactions with *P. aeruginosa*, but that quorum sensing molecules also play a crucial role in the attachment of *P. aeruginosa*. Differences in surface properties of bacteria vary the strength of adhesion on surfaces. Simoni et al. stated that the heterogeneity of LPS distribution in bacterial populations changes the adhesion characteristics [19].

When the information obtained from CLSM and AFM images is compared, CLSM gives lower resolution due to the limitations of light diffraction in optical microscopes whereas AFM can detect sub-nanometer size differences by the oscillations on the probe. It is important to note that AFM can produce artifacts on images. Depending on the shape of the tip and the height of the cells, it has been observed that the side of the probe can contact the cell and lead to misleading images. Thus the selection of the right tip shape to image bacteria is very crucial for accurate results [97].

### *3.4.6 Scanning Electron Microscopy (SEM)*

Scanning electron microscopy is another effective imaging tool that is used to elucidate biofilm structure and morphology [98]. Figure 3.9 shows a scanning electron micrograph of a *P. aeruginosa* biofilm formed on a polymer surface. An

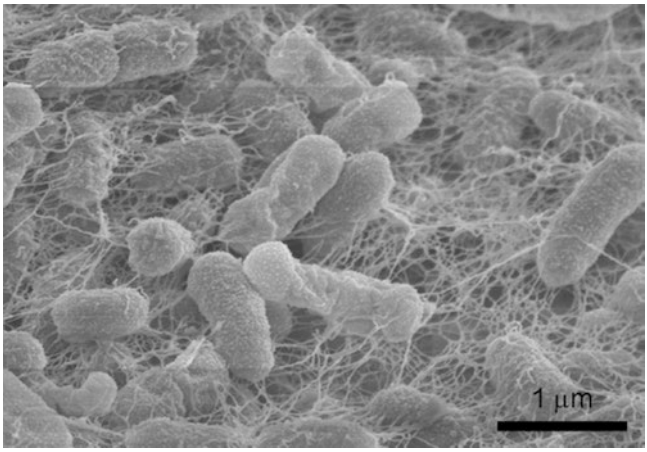


**Fig. 3.9** SEM image of a robust *P. aeruginosa* biofilm formed on a polydimethylsiloxane surface

interesting study was conducted by Wang and Libera (2013), which showed that biofilm formation can be inhibited by patterning the surface of a device. They took scanning electron micrographs (SEM) of patterned surfaces, which showed that when the size of the patches was smaller than 1 μm, the bacteria had trouble adhering to the surface [99]. They argued that when the *Staphylococcus aureus* tried to adhere to the surface, they were bent and curved by the pattern, which created a morphology that was energetically unfavorable for adhesion. The SEM images from the study showed that the patterned surfaces prevented adhesion and proliferation by showing groups of bacteria in biofilms on unpatterned surfaces, while there was a noticeable decrease in bacteria on the patterned surfaces. Their result suggests that biofilm formation can be reduced simply by changing the geometry of a surface. One major disadvantage of SEM imaging is the destructive sample preparation steps, which include the use of chemicals to fix and dehydrate the biofilm. The surface must also be conductive, which requires the deposition of a metal or other conductive coating. The preparation of the sample for SEM imaging can potentially alter the biofilm structure and bacterial morphology, so care must be taken during the process.

An alternative scanning electron microscopy has been introduced to improve the analysis of environmental species. Unlike SEM, environmental scanning electron microscopy (ESEM) runs at lower vacuum conditions, and the humidity can be controlled inside the chamber, which enables the maintenance of the sample properties in their original state [100, 101]. Though the resolution of ESEM is lower than SEM and the samples still must be coated with a conductive material, this technique is a very promising advancement for observing biofilm and the EPS structure [102].

### 3.4.7 Optical Tweezers

Optical tweezers are a scientific instrument that is used extensively to trap and manipulate single cells by focusing optical forces generated by photons in a laser beam to a certain location in a fluidic solution [103]. The cells can be inside of a channel as long as it is transparent. The refractive index mismatch between the cell and surrounding solution allows users to hold and move the cells. The light beam is focused by directing it through a microscope objective. The narrowest point of the focused beam contains a very strong electric field gradient. Dielectric particles, such as cells and proteins, are attracted along the gradient to the region of strongest electric field, which is located at the center of the beam.

Ashkin and Dziedzic demonstrated the ability to trap and move *E. coli* cells using optical tweezers for the first time in 1987 [104]. Other studies have utilized this method to analyze the adhesion forces between bacterial cells and surfaces [105]. Liang et al. implemented optical tweezers to orient *E. coli* cells and experimentally measure the forces required to detach the cells' pili from mannose groups on surfaces [54].

### 3.4.8 Microfluidics for Fluid Shear Stress Studies

Microfluidic technology has become a powerful tool for studying biofilms and bacterial cells. These miniaturized systems allow the observation of cells at single cell level by confining them to micrometer to sub-micrometer dimensions. There is an extensive body of literature describing the use of microfluidic devices to study biofilm formation along with excellent summaries of the topic [106]. Of particular relevance to biofilms is the use of microfluidics for shear stress analysis. Shear stress is known to remove biofilms, but recent research indicated that the relationship is likely much more complex. Lecuyer et al. showed that at early stages of adhesion, shear stress can increase the residence time of bacteria on the surface, inducing their attachment [107]. Thomas et al. elucidated that the attachment strength of *E. coli* cells to guinea pig erythrocytes increased tenfold upon exposure to shear stress [108]. Depending on cellular motility and the shear rate, shear stress has a trapping effect on cells, which can promote cell adhesion. Rusconi et al. highlighted that lower shear stress promotes cell accumulation around surface regions and induces biofilm formation [109]. Their experiments with *P. aeruginosa* PA14 demonstrated that the increase in shear stress led more surface attachment. This phenomenon becomes very critical in chronic infections seen with patients using medical devices such as catheters that incorporate fluid flow, which can induce this type of bacterial behavior. Another example of the shear stress effect on biofilm formation is seen with streamer bacteria. It is now known that bacteria form filamentous biofilms under certain flow conditions. To study this, a group of researchers designed a microfluidic device that contains zigzag-shaped channels to create vortices. At these

hydrodynamic regions, they observed the initial accumulation of polymeric substances and then the formation streamer biofilms around these regions [2, 3].

Park et al. (2011) used a polydimethylsiloxane (PDMS)-based microfluidic device to grow biofilms and assess the biofilm formation under a fluid shear. In the device, biofilms were formed by flowing bacteria into the device at varying shear stresses. Biofilm growth in the microfluidic devices was affected by the shear stress applied by the fluid containing the bacteria being deposited on the surface [110]. The study concluded that the time required to form a biofilm decreased as the velocity increased up to a threshold value, above which there was a sufficient shear force exerted such that the dissociation of the bacteria from the surface outweighed the increase in number of bacteria that reach the surface. They found that any shear stress applied in the device above 0.17 dyn/cm$^2$ (0.00017 mbar) would remove more bacteria than the flow added. This study demonstrated the mechanics of biofilm adhesion in fluid flow.

### *3.4.9 Raman Microscopy*

Raman microscopy is increasingly being utilized to map the spatial distribution of chemicals in biofilms. Raman microscopy provides chemical information about the material, via fingerprint spectra, in combination with the high spatial resolution by combining a Raman spectrometer with an optical microscope. Raman spectroscopy is a spectroscopic technique based on inelastic scattering of monochromatic light, usually from a laser source. Inelastic scattering means that the frequency of photons in monochromatic light changes upon interaction with a sample. The light beam from the spectrometer is focused onto the biofilm using the optics in the microscope. The photons are absorbed by the sample and then reemitted. The frequency of the reemitted photons is shifted up or down relative to the original monochromatic frequency, which is known as the Raman effect. This shift provides information about vibrational, rotational, and other low-frequency transitions in molecules. The light emitted back from the sample is collected and measured a charge-coupled device (CCD) or photomultiplier tube (PMT). Near-infrared (NIR) lasers are typically used for analyzing biological specimens as they emit lower energy light that is not as destructive to the sample. The main feature of this technique is that it requires little or no sample preparation as water has a very weak Raman signal [111].

Each molecule generates a unique Raman spectrum. Since biofilms contain thousands of different molecules, the complexity of sample does not allow for detailed chemical analysis, but concentration gradients can be mapped by looking at changes in the fingerprints obtained from different locations on the sample surface. This is done quantitatively with principal component analysis. One way to improve selectivity or sensitivity for this technique is to incorporate functionalized nanoparticles into the biofilm matrix that bind to targets of interest [112]. The best results are achieved by adding the nanoparticles during the biofilm formation process so that they can be incorporated uniformly.

### 3.4.10 Fourier Transform Infrared (FTIR) Spectroscopy

This technique is occasionally utilized to study biofilms. Infrared spectroscopy is performed by shining infrared light on the sample and measuring the absorbance of light in a range of wavelengths from 0.8 to 1000 micrometers. In FTIR, the absorbance information from all of the wavelengths is collected simultaneously to allow the information to be processed faster. Similar to Raman spectroscopy, FTIR instruments can be coupled with a microscope to image a sample surface. However, because of the intense absorption of infrared light by water, the biofilms are generally dried prior to imaging. To improve sensitivity, a special type of FTIR, known as attenuated total reflection (ATR), is generally utilized in these situations. As the name implies, ATR uses total reflection to guide the incident light along the sample surface, so that it can have more interaction with the sample than with the traditional setup, where the light travels through the sample. Using ATR, chemical information can be obtained from the sample even if it remains hydrated. One example of using FTIR spectroscopy was to measure diffusion of drug molecules through a fungal biofilm [113]. The chemical complexity of biofilm samples requires that fingerprinting or principle component analysis techniques be utilized to process the data similarly to Raman spectroscopy [114].

### 3.4.11 Surface Plasmon Resonance (SPR)

SPR sensors use a relatively simple instrument for measuring changes in biomass on a surface, but the phenomena employed in the measurement are quite complex. The most common instrument configuration has incident light shining on a prism made of high refractive index glass coated with 50 nm of gold [115, 116]. A microfluidic channel is attached over the gold surface to deliver solution to the sensor surface. At a certain angle, referred to as the resonance angle, the photons from the incident light entering the prism are transferred to the free electrons in the metal creating surface plasmon polaritons (SPPs) that extend approximately 200 nm above the surface. In this state, no light is reflected back out from the prism. When biomass, such as bacterial cells or extracellular matrix, attaches to the gold, the water on the surface is displaced, the refractive index is changed, the SPPs cannot form, and the incident light is reflected back out of the prism. The amount of reflected light is measured with a CCD. The intensity of the light is proportional to the amount of biomass on the sensor surface.

SPR has been used to study the adhesion of *P. aeruginosa* on bare and modified gold surfaces [117]. The results of these experiments showed that differences in binding kinetics could be distinguished for different surfaces and strains of cells. SPR is being used to determine the binding mechanisms of bacterial species by testing their adhesion kinetics to various natural and synthetic materials [118, 119]. SPR is being tested in pilot plants to detect biofilm formation on reactor surfaces [120].

### 3.4.12 Surface Plasmon Resonance Imaging (SPRi)

In a traditional SPR system, the average intensity of the reflected light from the entire surface is measured, and the results show the average refractive index variation of the sample on the entire surface. In SPR imaging, the intensity of the reflected light is analyzed at each position on the sensing surface. The output of this sensor is a grayscale image, which is called difference image and represents the refractive index changes of the dielectric media above the metal film pixel by pixel (Fig. 3.10). The pixel size determines the resolution of the device.

SPRi offers the unique advantages of measuring attachment of molecules onto a surface accompanied by large area imaging (~1 $cm^2$) [122, 123]. No other technique can provide these two attributes simultaneously, which are vitally important for investigating biofilm formation and removal [124]. The large area is necessary because the simultaneous movement of hundreds or thousands of cells, as well as the insoluble polysaccharides and proteins excreted by the cells, in a biofilm must be tracked during each stage of the biofilm life cycle [125]. Its simplicity, rapid analysis, low cost compared to confocal microscopy, and potential miniaturization [126, 127] make it an ideal technique for studying biofilm formation and decomposition in clinical and industrial environments.

The use of both SPR and SPRi for bacterial analysis is becoming increasingly prevalent [128]. The rapid imaging capabilities of a SPRi system are particularly important for multicellular and bacterial movement investigations. By using chambers and channels that confine cells near the sensor surface, it is possible to observe physical activity inside the chambers, such as cell movement and growth [123]. Even though the cells are much larger than the approximately 200 nm electromagnetic field that extends from the sensor surface, a significant portion of the cell is located within the field and is detected. Abadian et al. [129, 121] exploited this fact

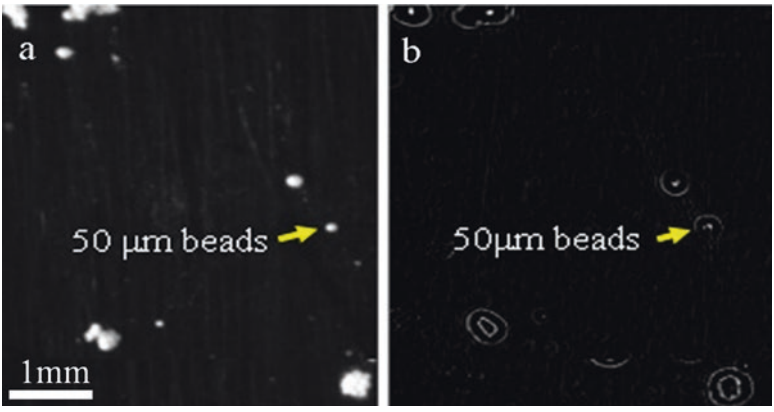


**Fig. 3.10** (**a**) A microscope image of 50 µm beads on the prism surface. (**b**) The SPRi difference image from the same surface. The bright spots are where beads attached the surface and changed the refractive index at those locations (Adapted from Ref. [121])

to image the movement, adhesion, and removal of cells in biofilms in real time at the sensor surface. At the end of each experiment, the PDMS made chamber was removed and sensor surfaces were analyzed using fluorescence microscopy and scanning electron microscopy.

### *3.4.13 Quartz Crystal Microbalance (QCM)*

Another approach for analysis of biofilm formation and removal is to use a quartz crystal microbalance. Very simply, quartz crystal microbalance (QCM) sensors measure the mass attached to a surface using changes in vibrational frequency. Applying an alternating current to quartz crystal sandwiched between two electrodes induces oscillations through the crystal in the direction parallel to the electrodes (known as a shear wave). The alternating current can be selected such that it matches the natural frequency of the crystal, thus generating a resonant frequency in the megahertz range. The frequency at which the sensor oscillates changes as mass is added or removed.

Frequency measurements are easily made with high precision; hence, it is easy to measure mass densities on the sensor surface that are as low as 1 μg/cm$^2$. When working with liquids, it is important to also measure the dissipation factor to help in the analysis and the viscoelastic properties of the liquid affect the sensor performance and the mass density it measures. Figure 3.11 shows a schematic of the sensor.

There is a substantial amount of work demonstrating the ability to use QCM as a biosensor to detect the presence of bacteria [130]; however, we are focused on characterization of biofilms. Nivens et al. measured the rate of biofilm formation for *Pseudomonas cepacia* using a QSM [131]. Castro et al. investigated the growth of *S. epidermidis* biofilms using a QCM sensor [132]. They observed that the dissipation factor, which is equivalent to the resonance bandwidth, increased dramatically for a mutant strain that did not produce extracellular matrix, while wild-type strains forming robust biofilms caused smaller changes. The mutant strain also caused the greatest frequency shift. Reipa et al. coupled QCM with optical detection to simultaneously measure changes in the viscoelastic properties and thickness of the biofilm in real time over the course of several days [133].

More recently, Ollson et al. used a QCM with dissipation (QCM-D) to determine the effect that bacterial appendages have on these types of measurements [134].

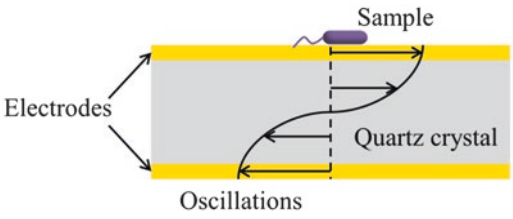


**Fig. 3.11** Schematic demonstrating the sensing principle of a QCM

They found that bacteria devoid of surface appendages registered a frequency decrease. Adhesion of bacteria possessing surface appendages yielded either a smaller decrease or even an increase in frequency, despite the fact that more cells adhered. Vanoyan et al. measured changes in bacterial deposition and attachment when the cells were exposed to molecules inhibiting quorum sensing [135].

## 3.5 Final Remarks

There are many analytical methods available for characterizing bacterial cell adhesion and biofilms, but care has to be taken to select the appropriate approach for the particular property that is being investigated. The dynamic and highly variable properties of biofilms also require that experimental conditions mimic, as precisely as possible, the natural environment where the biofilm is found. Existing techniques are also frequently combined to provide a more accurate representation of the biofilm properties. It is expected that additional techniques will be developed in the future as the importance of biofilms is realized throughout the scientific community.

## References

1. R.M. Donlan, Biofilms: microbial life on surfaces. Emerg. Infect. Dis. **8**, 881–890 (2002)
2. R. Rusconi, S. Lecuyer, L. Guglielmini, H.A. Stone, Laminar flow around corners triggers the formation of biofilm streamers. J. R. Soc. Interface **7**, 1293–1299 (2010)
3. R. Rusconi, S. Lecuyer, N. Autrusson, L. Guglielmini, A. Stone Howard, Secondary flow as a mechanism for the formation of Biofilm streamers. Biophys. J. **100**, 1392–1399 (2011)
4. P.G. Falkowski, T. Fenchel, E.F. DeLong, The microbial engines that drive Earth's biogeochemical cycles. Sci **320**, 1034–1039 (2008)
5. W.G. Zumft, Cell biology and molecular basis of denitrification. Microbiol. Mol. Biol. Rev. **61**, 533–616 (1997)
6. J. Vymazal, Removal of nutrients in various types of constructed wetlands. Sci. Total Environ. **380**, 48–65 (2007)
7. C.J. Richardson, Mechanisms controlling phosphorus retention capacity in freshwater wetlands. Sci **228**, 1424–1427 (1985)
8. W.M. Dunne, Bacterial adhesion: seen any good Biofilms lately? Clin. Microbiol. Rev. **15**, 155–166 (2002)
9. L. Hall-Stoodley, J.W. Costerton, P. Stoodley, Bacterial biofilms: from the natural environment to infectious diseases. Nat. Rev. Microbiol. **2**, 95–108 (2004)
10. P. Stoodley, K. Sauer, D.G. Davies, J.W. Costerton, Biofilms as complex differentiated communities. Annu. Rev. Microbiol. **56**, 187–209 (2002)
11. H.J. Busscher, H.C. Van der Mei, How do bacteria know they are on a surface and regulate their response to an adhering state. PLoS Pathog. **8**, e1002440 (2012)
12. H.H. Tuson, D.B. Weibel, Bacteria-surface interactions. Soft Matter **9**, 4368–4380 (2013)
13. R. Bos, H.C. Van der Mei, H.J. Busscher, Physico-chemistry of initial microbial adhesive interactions- its mechanisms and methods for study. FEMS Microbiol. Rev. **23**, 179–230 (1999)
14. H. Wang, M. Sodagari, Y. Chen, X. He, B.M. Newby, et al., Initial bacterial attachment in slow flowing systems: effects of cell and substrate surface properties. Colloids Surf. B Biointerfaces **87**, 415–422 (2011)

15. Y. Liu, J. Strauss, T.A. Camesano, Thermodynamic investigation of *Staphylococcus epidermis* interactions with protein-coated substrata. Langmuir **23**, 7134–7142 (2007)
16. M.E. Schrader, Young-dupre revisited. Langmuir **11**, 3585–3589 (1995)
17. N.P. Boks, W. Norde, H.C. van der Mei, H.J. Busscher, Forces involved in bacterial adhesion to hydrophilic and hydrophobic surfaces. Microbiology **154**, 3122–3133 (2008)
18. M.C.M. Van Loosdrecht, J. Lyklema, W. Norde, A.J.B. Zehnder, Influence of interfaces on microbial activity. Microbiol. Rev. **54**, 75–87 (1990)
19. S.F. Simoni, H. Harms, T.N.P. Bosma, A.J.B. Zehnder, Population heterogeneity affects transport of bacteria through sand columns at low flow rates. Environ. Sci. Technol. **32**, 2100–2105 (1998)
20. M.C.M. Van Loosdrecht, J. Lyklema, W. Norde, A.J.B. Zehnder, Bacterial adhesion: a physicochemical approach. Microb. Ecol. **17**, 1–15 (1989)
21. J.T. Gannon, V.B. Manilal, M. Alexander, Relationship between cell surface properties and transport of bacteria through soil. Appl. Environ. Microbiol. **57**, 190–193 (1991)
22. T.J. Silhavy, D. Kahne, S. Walker, The bacterial cell envelope. Cold Spring Harb. Perspect. Biol. **2**, a000414 (2010)
23. M. Hermansson, The DLVO theory in microbial adhesion. Colloids Surf. B: Biointerfaces **14**, 105–119 (1999)
24. K. Hori, S. Matsumoto, Bacterial adhesion: from mechanism to control. Biochem. Eng. J. **48**, 424–434 (2010)
25. J.A. Redman, S.L. Walker, M. Elimelech, Bacterial adhesion and transport in porous media: role of the secondary energy minimum. Environ. Sci. Technol. **38**, 1777–1785 (2004)
26. H.H.M. Rijnaarts, W. Norde, E.J. Bouwer, J. Lyklema, A.J.B. Zehnder, Reversibility and mechanism of bacterial adhesion. Colloids Surf. B: Biointerfaces **4**, 5–22 (1995)
27. A. Zita, M. Hermansson, Effects of bacterial cell surface structures and Hydrophobicity on attachment to activated sludge Flocs. Appl. Environ. Microbiol. **63**, 1168–1170 (1997)
28. A. Zita, M. Hermansson, Determination of bacterial cell surface hydrophobicity of single cells in cultures and in wastewater in situ. FEMS Microbiol. Lett. **152**, 299–306 (1997)
29. M.C.M. van Loosdrecht, J. Lyklema, W. Norde, G. Schraa, A.J.B. Zehnder, Electrophoretic mobility and hydrophobicity as a measured to predict the initial steps of bacterial adhesion. Appl. Environ. Microbiol. **53**, 1898–1901 (1987)
30. M. Morra, C. Cassinelli, Bacterial adhesion to polymer surfaces: a critical review of surface thermodynamic approaches. J. Biomater. Sci. Polym. Ed. **9**, 55–74 (1998)
31. W. Qu, H.J. Busscher, J.M. Hooymans, H.C. van der Mei, Surface thermodynamics and adhesion forces governing bacterial transmission in contact lens related microbial keratitis. J. Colloid Interface Sci. **358**, 430–436 (2011)
32. S. McEldowney, M. Fletcher, Variablity of the influence of Physicochemical factors affecting bacterial adhesion to polystyrene Subsrata. Appl. Environ. Microbiol. **52**, 460–465 (1986)
33. P.K. Sharma, K. Hanumantha Rao, Adhesion of Paenibacillus polymyxa on chalcopyrite and pyrite: surface thermodynamics and extended DLVO theory. Colloids Surf. B: Biointerfaces **29**, 21–38 (2003)
34. L.S. Dorobantu, S. Bhattacharjee, J.M. Foght, M.R. Gray, Analysis of force interactions between AFM tips and hydrophobic bacteria using DLVO theory. Langmuir **25**, 6968–6976 (2009)
35. G. Hwang, I.S. Ahn, B.J. Mhin, J.Y. Kim, Adhesion of nano-sized particles to the surface of bacteria: mechanistic study with the extended DLVO theory. Colloids Surf. B: Biointerfaces **97**, 138–144 (2012)
36. C. Van Oss, Energetics of cell-cell and cell-biopolymer interactions. Cell Biophys. **14**, 1–16 (1989)
37. Y.-L. Ong, A. Razatos, G. Georgiou, M.M. Sharma, Adhesion forces between *E. coli* bacteria and biomaterial surfaces. Langmuir **15**, 2719–2725 (1999)
38. I. Banerjee, R.C. Pangule, R.S. Kane, Antifouling coatings: recent developments in the design of surfaces that prevent fouling by proteins, bacteria, and marine organisms. Adv. Mater. **23**, 690–718 (2011)

39. D.R. Monteiro, L.F. Gorup, A.S. Takamiya, A.C. Ruvollo-Filho, E.R. de Camargo, et al., The growing importance of materials that prevent microbial adhesion: antimicrobial effect of medical devices containing silver. Int. J. Antimicrob. Agents **34**, 103–110 (2009)
40. R.P. Allaker, The use of nanoparticles to control oral biofilm formation. J. Dent. Res. **89**, 1175–1186 (2010)
41. M.L.W. Knetsch, L.H. Koole, New strategies in the development of antimicrobial coatings: the example of increasing usage of silver and silver Nanoparticles. Polymer **3**, 340–366 (2011)
42. L.K. Ista, H. Fan, O. Baca, G.P. Lopez, Attachment of bacteria to model solid surfaces: oligo (ethylene glycol) surfaces inhibit bacterial attachment. FEMS Microbiol. Lett. **142**, 59–63 (1996)
43. E. Ostuni, R.G. Chapman, M.N. Liang, G. Meluleni, G. Pier, D.E. Ingber, G.M. Whitesides, Self-assembled Monolayers that resist the adsorption of proteins and the adhesion of bacterial and mammalian cells. Langmuir **17**, 6336–6343 (2001)
44. H.C. Flemming, J. Wingender, The biofilm matrix. Nat. Rev. Microbiol. **8**, 623–633 (2010)
45. G. O'Toole, H.B. Kaplan, R. Kolter, Biofilm formation as microbial development. Annu. Rev. Microbiol. **54**, 49–79 (2000)
46. J. Kim, H.D. Park, S. Chung, Microfluidic approaches to bacterial biofilm formation. Molecules **17**, 9818–9834 (2012)
47. J.L. Connell, A.K. Wessel, M.R. Parsek, A.D. Ellington, M. Whiteley, J.B. Shear, Probing prokaryotic social behaviors with bacterial "lobster traps". MBio **1**(4), e00202–e00210 (2010)
48. D.G. Davies, M.R. Parsek, J.P. Pearson, B.H. Iglewski, J.W. Costerton, E.P. Greenberg, The involvement of cell-to-cell signals in the development of a bacterial Biofilm. Science **280**, 295–298 (1998)
49. D.G. Davies, A.M. Chakrabarty, G.G. Geesey, Exopolysaccharide production in biofilms: Substratum activation of alginate gene expression by *Pseudomonas aeruginosa*. Appl. Environ. Microbiol. **59**, 1181–1186 (1993)
50. D.G. Davies, G.G. Geesey, Regulation of the alginate biosynthesis Gene *algC* in *Pseudomonas aeruginosa* during Biofilm development in continuous culture. Appl. Environ. Microbiol. **61**, 860–867 (1995)
51. O. Bahar, L. De La Fuente, S. Burdman, Assessing adhesion, biofilm formation and motility of Acidovorax citrulli using microfluidic flow chambers. FEMS Microbiol. Lett. **312**, 33–39 (2010)
52. A. Perry, I. Ofek, F.J. Silverblatt, Enhancement of mannose-mediated stimulation of human granulocytes by type 1 Fimbriae aggregated with antibodies on *Escherichia coli* surfaces. Infect. Immun. **39**, 1334–1345 (1983)
53. S.N. Abraham, D. Sun, J.B. Dale, E.H. Beachey, Conservation of the D-mannose-adhesion protein among type 1 fimbriated members of the family Enterobacteriaceae. Nature **336**, 682–684 (1988)
54. M.N. Liang, S.P. Smith, S.J. Metallo, I.S. Choi, M. Prentiss, G.M. Whitesides, Measuring the forces involved in polyvalent adhesion of uropathogenic *Escherichia coli* to mannose-presenting surfaces. Proc. Natl. Acad. Sci. U. S. A. **97**, 13092–13096 (2000)
55. K.A. Krogfelt, H. Bergmans, P. Klemm, Direct evidence that the FimH protein is the mannose-specific Adhesin of *Escherichia coli* type 1 Fimbriae. Infect. Immun. **58**, 1995–1998 (1990)
56. S.H. Hong, M. Hegde, J. Kim, X. Wang, A. Jayaraman, T.K. Wood, Synthetic quorum-sensing circuit to control consortial biofilm formation and dispersal in a microfluidic device. Nat. Commun. **3**, 613 (2012)
57. K. Lewis, Persister cells and the riddle of Biofilm survival. Biochem. Mosc. **70**, 267–274 (2005)
58. K. Sauer, A.K. Camper, G.D. Ehrlich, J.W. Costerton, D.G. Davies, Pseudomonas Aeruginosa displays multiple phenotypes during development as a Biofilm. J. Bacteriol. **184**, 1140–1154 (2002)

59. I. Kolodkin-Gal, S. Cao, L. Chai, T. Bottccher, R. Kolter, J. Clardy, R. Losick, A self-produced trigger for biofilm disassembly that targets exopolysaccharide. Cell **149**(3), 684–692 (2012)
60. CBE milestones: An abbreviated timeline. Retrieved 20 Apr 2015., from https://www.biofilm.montana.edu/cbe-milestones-abbreviated-timeline.html
61. N. Zelver, M. Hamilton, B. Pitts, D. Goeres, D. Walker, P. Sturman, J. Heersink, Measuring antimicrobial effects on Biofilm bacteria: from laboratory to field. Methods Enzymol. **310**, 608–628 (1999)
62. ASTM E2562–12 Standard test method for quantification of Pseudomonas aeruginosa Biofilm grown with high shear and continuous flow using CDC Biofilm reactor, (2012), Retrieved 20 Apr 2015, from http://www.astm.org/Standards/E2562.htm
63. D.L. Williams, K.L. Woodbury, B.S. Haymond, A.E. Parker, R.D. Bloebaum, A modified CDC Biofilm reactor to produce mature Biofilms on the surface of PEEK membranes for an in vivo animal model application. Curr. Microbiol. **62**(6), 1657–1663 (2011)
64. ASTM E2647–13 Standard test method for quantification of Pseudomonas aeruginosa Biofilm grown using Drip Flow Biofilm reactor with low shear and continuous flow, (2013), Retrieved 20 Apr 2015, from http://www.astm.org/Standards/E2647.htm
65. Y. Liu, J.H. Tay, Metabolic response of biofilm to shear stress in fixed-film culture. J. Appl. Microbiol. **90**(3), 337–342 (2001)
66. A.P. Foncesa, J.C. Sousa, Effect of shear stress on growth, adhesion and biofilm formation of Pseudomonas Aeruginosa with antibiotic-induced morphological changes. Int. J. Antimicrob. Agents **30**(3), 236–241 (2007)
67. H. Ceri, M.E. Olson, C. Stremick, R.R. Read, D. Morck, A. Buret, The Calgary Biofilm device: new technology for rapid determination of antibiotic susceptibilities of bacterial Biofilms. J. Clin. Microbiol. **37**(6), 1771–1776 (1999)
68. L. Santopolo, E. Marchi, L. Frediani, F. Decorosi, C. Viti, L. Giovannetti, A novel approach combining the Calgary Biofilm device and phenotype MicroArray for the characterization of the chemical sensitivity of bacterial biofilms. Biofouling **28**(9), 1023–1032 (2012)
69. Y.C. Choi, E. Morgenroth, Monitoring biofilm detachment under dynamic changes in shear stress using laser-based particle size analysis and mass fractionation. Water Sci. Technol. **47**(5), 69–76 (2013)
70. E.L. Decker, B. Frank, Y. Suo, S. Garoff, Physics of contact angle measurement. Colloids Surf. A Physicochem. Eng. Asp. **156**, 177–189 (1999)
71. D. Daffonchio, J. Thaveesri, W. Verstraete, Contact angle measurement and cell Hydrophobicity of granular sludge from upflow anaerobic sludge bed reactors. Appl. Environ. Microbiol. **61**, 3676–3680 (1995)
72. Y.C. Jung, B. Bhushan, Technique to measure contact angle of micro/nanodroplets using atomic force microscopy. J. Vac. Sci. Technol. A **26**, 777 (2008)
73. A.M. Gallardo-Moreno, M.L. Navarro-Perez, V. Vadillo-Rodriguez, J.M. Bruque, M.L. Gonzalez-Martin, Insights into bacterial contact angles: difficulties in defining hydrophobicity and surface Gibbs energy. Colloids Surf. B: Biointerfaces **88**(1), 373–380 (2011)
74. R.J. Palmer Jr., C. Sternberg, Modern microscopy in Biofilm research: confocal microscopy and other approaches. Curr. Opin. Biotechnol. **10**, 263–268 (1999)
75. M. Fletcher, Bacterial biofilms and biofouling. Curr. Opin. Biotechnol. **5**, 302–306 (1994)
76. M. Ferrando, W.E.L. Spiess, Review: confocal scanning laser microscopy. A powerful tool in food science. Food Sci. Technol. Int. **6**, 267–284 (2000)
77. Y. Yawata, K. Toda, E. Setoyama, J. Fukuda, H. Suzuki, H. Uchiyama, N. Nomura, Monitoring biofilm development in a microfluidic device using modified confocal reflection microscopy. J. Biosci. Bioeng. **110**, 377–380 (2010)
78. J.R. Lawrence, D.R. Korber, B.D. Hoyle, J.W. Costerton, D.E. Caldwell, Optical sectioning of microbial Biofilms. J. Bacteriol. **173**, 6558–6567 (1991)
79. D.E. Caldwell, D.R. Korber, J.R. Lawrence, Imaging of bacterial cells by fluorescence exclusion using scanning confocal laser microscopy. J. Microbiol. Methods **15**, 249–261 (1992)
80. D.E. Caldwell, D.R. Korber, J.R. Lawrence, Analysis of biofilm formation using 2D vs 3D digital imaging. J. Appl. Bacteriol. **74**, 52S–66S (1993)

81. S.R. Wood, J. Kirkham, P.D. Marsh, R.C. Shore, B. Nattress, et al., Architecture of intact natural human plaque Biofilms studied by Confocal laser scanning microscopy. J. Dent. Res. **79**, 21–27 (2000)
82. J. Kim, B. Pitts, P.S. Stewart, A. Camper, J. Yoon, Comparison of the antimicrobial effects of chlorine, silver ion, and Tobramycin on Biofilm. Antimicrob. Agents Chemother. **52**, 1446–1453 (2008)
83. C. Staudt, H. Horn, D.C. Hempel, T.R. Neu, Volumetric measurements of bacterial cells and extracellular polymeric substance glycoconjugates in biofilms. Biotechnol. Bioeng. **88**, 585–592 (2004)
84. T. Bjarnsholt, P.O. Jensen, M.J. Fiandaca, J. Pedersen, C.R. Hansen, C.B. Andersen, T. Pressler, M. Givskov, N. Hoiby, *Pseudomonas aeruginosa* biofilms in the respiratory tract of cystic fibrosis patients. Pediatr. Pulmonol. **44**, 547–558 (2009)
85. A. Touhami, M.H. Jericho, T.J. Beveridge, Atomic force microscopy of cell growth and division in *Staphylococcus aureus*. J. Bacteriol. **186**, 3286–3295 (2004)
86. H.H.P. Fang, K.-Y. Chan, L.-C. Xu, Quantification of bacterial adhesion forces using atomic force microscopy (AFM). J. Microbiol. Methods **40**, 89–97 (2000)
87. T.A. Camesano, M.J. Natan, B.E. Logan, Observation of changes in bacterial cell morphology using tapping mode atomic force microscopy. Langmuir **16**, 4563–4572 (2000)
88. C.J. Wright, M.K. Shah, L.C. Powell, I. Armstrong, Application of AFM from microbial cell to biofilm. Scanning **32**, 134–149 (2010)
89. Y.F. Dufrene, Atomic force microscopy, a powerful tool in microbiology. J. Bacteriol. **184**, 5205–5213 (2002)
90. D. Fotiadis, S. Scheuring, S.A. Müller, A. Engel, D.J. Müller, Imaging and manipulation of biological structures with the AFM. Micron **33**, 385–397 (2002)
91. M. Quirynen, C.M.L. Bollen, The influence of surface roughness and surface-free energy on supra- and subgingival plaque formation in man. J. Clin. Periodontol. **22**, 1–14 (1995)
92. H.J. Busscher, M. Rinastiti, W. Siswomihardjo, H.C. van der Mei, Biofilm formation on dental restorative and implant materials. J. Dent. Res. **89**, 657–665 (2010)
93. R. Burgers, W. Schneider-Brachert, M. Rosentritt, G. Handel, S. Hahnel, *Candida albicans* Adhesion to composite resin materials. Clin. Oral Investig. **13**, 293–299 (2009)
94. M. Quirynen, M. Marechal, D. Van Steenberghe, H.J. Busscher, H.C. Van Der Mei, The bacterial colonization of intra-oral hard surfaces in vivo: influence of surface free energy and surface roughness. Biofouling **4**, 187–198 (1991)
95. L. Mei, H.J. Busscher, H.C. van der Mei, Y. Ren, Influence of surface roughness on streptococcal adhesion forces to composite resins. Dent. Mater. **27**, 770–778 (2011)
96. E.S. Ovchinnikova, B.P. Krom, H.C. van der Mei, H.J. Busscher, Force microscopic and thermodynamic analysis of the adhesion between Pseudomonas Aeruginosa and *Candida albicans*. Soft Matter **8**, 6454–6461 (2012)
97. S.B. Velegol, S. Pardi, X. Li, D. Velegol, B.E. Logan, AFM imaging artifacts due to bacterial cell height and AFM tip geometry. Langmuir **19**, 851–857 (2003)
98. P. Chavant, B. Gaillard-Martinie, R. Talon, M. Hebraud, T. Bernardi, A new device for rapid evaluation of biofilm formation potential by bacteria. J. Microbiol. Methods **68**, 605–612 (2007)
99. Y. Wang, M. Libera, *Length-Scale Effects on the Differential Adhesion of Bacteria and Mammalian Cells* (ProQuest LLC, 2013)
100. T. Schwartz, C. Jungfer, S. Heissler, F. Friedrich, W. Faubel, et al., Combined use of molecular biology taxonomy, Raman spectrometry, and ESEM imaging to study natural biofilms grown on filter materials at waterworks. Chemosphere **77**, 249–257 (2009)
101. L. Bergmans, P. Moisiadis, B. Van Meerbeek, M. Quirynen, P. Lambrechts, Microscopic observation of bacteria: review highlighting the use of environmental SEM. Int. Endod. J. **38**, 775–778 (2005)
102. J.H. Priester, A.M. Horst, L.C. Van De Werfhorst, J.L. Saleta, L.A.K. Mertes, et al., Enhanced visualization of microbial Biofilms by staining and environmental scanning electron microscopy. J. Microbiol. Methods **68**, 577–587 (2007)

103. M. Ericsson, D. Hanstorp, P. Hagberg, J. Enger, T. Nystrom, Sorting out bacterial viability with optical tweezers. J. Bacteriol. **182**, 5551–5555 (2000)
104. A. Ashkin, J.M. Dziedzic, Optical trapping and manipulation of viruses and bacteria. Science **235**(4795), 1517–1520 (1987)
105. H. Zhang, K.K. Liu, Optical tweezers for single cells. J. R. Soc. Interface **5**(24), 671–690 (2008)
106. F.J.H. Hol, C. Dekker, Zooming in to see the bigger picture: microfluidic and nanofabrication tools to study bacteria Felix. Science **346**(6208), 402–403 (2014)
107. S. Lecuyer, R. Rusconi, Y. Shen, A. Forsyth, H. Vlamakis, R. Kolter, H.A. Stone, Shear stress increases the residence time of adhesion of *Pseudomonas aeruginosa*. Biophys. J. **100**, 341–350 (2011)
108. W.E. Thomas, E. Trintchina, M. Forero, V. Vogel, E.V. Sokurenko, Bacterial adhesion to target cells enhanced by shear force. Cell **109**, 913–923 (2002)
109. R. Rusconi, J.S. Guasto, R. Stocker, Bacterial transport suppressed by fluid shear. Nat. Phys. **10**, 212–217 (2014)
110. A. Park, H.H. Jeong, J. Lee, K.P. Kim, C.S. Lee, Effect of shear stress on the formation of bacterial biofilm in a microfluidic channel. Biochip J. **5**(3), 236–241 (2011)
111. N.P. Ivleva, M. Wagner, H. Horn, R. Niessner, C. Haisch, Towards a nondestructive chemical characterization of biofilm matrix by Raman microscopy. Anal. Bioanal. Chem. **393**(1), 197–206 (2009)
112. Y. Chao, T. Zhang, Surface-enhanced Raman scattering (SERS) revealing chemical variation during biofilm formation: from initial attachment to mature biofilm. Anal. Bioanal. Chem. **404**(5), 1465–1475 (2012)
113. P.A. Suci, G.G. Geesey, B.J. Tyler, Integration of Raman microscopy, differential interference contrast microscopy, and attenuated total reflection fourier transform infrared spectroscopy to investigate chlorhexidine spatial and temporal distribution in *Candida albicans* biofilms. J. Microbiol. Methods **46**, 193–208 (2001)
114. F. Humbert, F. Quiles, A. Delille, in *Proceedings of the II International Conference on Environmental, Industrial and Applied Microbiology (BioMicroWorld2007) Current Research Topics in Applied Microbiology and Microbial Biotechnology*, ed. by A Mendez-Vilas. In situ assessment of drinking water biostability using nascent reference biofilm ATR-FTIR fingerprint, (World Scientic Publishing Co. Pte. Ltd., Singapore, 2009), p. 268–272
115. K. Aslan, C.D. Geddes, Directional surface Plasmon coupled luminescence for analytical sensing applications: which metal, what wavelength, what observation angle? Anal. Chem. **81**, 6913–6922 (2009)
116. A.G. Koutsioubas, N. Spiliopoulos, D. Anastassopoulos, A.A. Vradis, G.D. Priftis, Nanoporous alumina enhanced surface plasmon resonance sensors. J. Appl. Phys. **103**, 094521–094526 (2008)
117. A.T.A. Jenkins, R. ffrench-constant, A. Buckling, D.J. Clarke, K. Jarvis, Study of the attachment of Pseudomonas Aeruginosa on gold and modified gold surfaces using surface Plasmon resonance. Biotechnol. Prog. **20**, 1233–1236 (2004)
118. J. Landrygan-Bakri, M.J. Wilson, D.W. Williams, M.A. Lewis, R.J. Waddington, Real-time monitoring of the adherence of *Streptococcus anginosus* group bacteria to extracellular matrix decorin and biglycan proteoglycans in biofilm formation. Res. Microbiol. **163**, 436–447 (2012)
119. A. Pranzetti, S. Salaün, S. Mieszkin, M.E. Callow, J.A. Callow, J.A. Preece, P.M. Mendes, Model organic surfaces to probe marine bacterial adhesion kinetics by surface Plasmon resonance. Adv. Funct. Mater. **22**, 3672–3681 (2012)
120. P. Janknecht, L. Melo, Online Biofilm monitoring. Rev. Environ. Sci. Biotechnol. **2**, 269–283 (2003)
121. P.N. Abadian, N. Tandogan, T.A. Webster, E.D. Goluch, Real-time detection of bacterial biofilm growth using surface plasmon resonance. *16th International Conference on Miniaturized Systems for Chemistry and Life Sciences* (microTAS 2012), (Okinawa, JP, 2012), pp. 413–415

122. S. Paul, P. Vadgama, A.K. Ray, Surface plasmon resonance imaging for biosensing. Nanobiotechnol. IET **3**, 71–80 (2009)
123. Y. Yanase, T. Hiragun, S. Kaneko, H.J. Gould, M.W. Greaves, M. Hide, Detection of refractive index changes in individual living cells by means of surface plasmon resonance imaging. Biosens. Bioelectron. **26**, 674–681 (2010)
124. K. Marion-Ferey, M. Pasmore, P. Stoodley, S. Wilson, G.P. Husson, J.W. Costerton, Biofilm removal from silicone tubing: an assessment of the efficacy of dialysis machine decontamination procedures using an in vitro model. J. Hosp. Infect. **53**, 64–71 (2003)
125. J.D. Chambless, S.M. Hunt, P.S. Stewart, A three-dimensional computer model of four hypothetical mechanisms protecting Biofilms from antimicrobials. Appl. Environ. Microbiol. **72**, 2005–2013 (2006)
126. R.D. Harris, J.S. Wilkinson, Waveguide surface plasmon resonance sensors. Sensors Actuators B Chem. **29**, 261–267 (1995)
127. A. Karabchevsky, L. Tsapovsky, R.S. Marks, I. Abdulhalim, Optical immunosensor for endocrine disruptor nanolayer detection by surface plasmon resonance imaging. Proc. SPIE 8099, Biosensing and Nanomedicine IV: 809918 (2011)
128. P.N. Abadian, C.P. Kelley, E.D. Goluch, Cellular analysis and detection using surface Plasmon resonance techniques. Anal. Chem. **86**, 2799–2812 (2014)
129. P.N. Abadian, N. Tandogan, J.J. Jamieson, E.D. Goluch, Using surface plasmon resonance imaging to study bacterial biofilms. Biomicrofluidics **8**, 021804 (2014)
130. N.A. Saad, S.K. Zaaba, A. Zakaria, L.M. Kamarudin, K. Wan, A.B. Shariman, Quartz crystal microbalance for bacteria application review. *2nd International Conference on Electronic Design* (*ICED*), (Penang, 2014), pp. 455–460
131. D.E. Nivens, J.Q. Chambers, T.R. Anderson, D.C. White, Long-term, on-line monitoring of microbial biofilms using a quartz crystal microbalance. Anal. Chem. **61**(1), 65–69 (1993)
132. P. Castro, P. Resa, C. Durán, J.R. Maestre, M. Mateo, L. Elvira, Continuous monitoring of bacterial biofilm growth using uncoated thickness-shear mode resonators. IOP Conf. Ser. Mater. Sci. Eng **42**, 012054 (2012)
133. V. Reipa, J. Almeida, K.D. Cole, Long-term monitoring of biofilm growth and disinfection using a quartz crystal microbalance and reflectance measurements. J. Microbiol. Methods **66**, 449–459 (2006)
134. A.L.J. Olsson, H.C. van der Mei, H.J. Busscher, P.K. Sharma, Influence of cell surface appendages on the bacterium substratum Interface measured real-time using QCM-D. Langmuir **25**, 1627–1632 (2009)
135. N. Vanoyan, S.L. Walker, O. Gillor, M. Herzberg, Reduced bacterial deposition and attachment by quorum sensing inhibitor 4-nitro-pyridine-N-oxide: the role of Physicochemical effects. Langmuir **26**, 12089–12094 (2010)